DEVELOPING CRISM METHODS FOR FINDING HYDROUS CHLORIDES ON MARS

Sharissa. Y. Thompson[1] and Martha S. Gilmore[2], [1]Dept. Of Earth and Atmospheric Sciences, Georgia Institute of Technology, Atlanta, GA 30332, USA (Contact: sthompson318@gatech.edu), [2]Dept. of Earth and Environmental Sciences, Wesleyan University, Middletown, CT 06459, USA.

Introduction: Putative anhydrous chloride deposits (Fig. 1) have been detected in previous studies using thermal infrared (TIR) images from the Thermal Imaging Emission System (THEMIS) on the Mars Odyssey Orbiter [1], VNIR data on MRO [2] and by ChemCam on the Curiosity rover [3]. These chloride deposits may record aqueous environments occurring historically in the Noachian period on Mars [1]. These deposits commonly occur in topographically low regions and leveled intercrater plains or crater basins in the southern highlands of Mars [1,2,4]. Anhydrous chlorides lack definitive spectral absorptions in the VNIR and TIR and thus their detection is based on general spectral shape [1, 5, 6]. However, hydrous chlorides, which are expected to develop in evaporite deposits, do have diagnostic spectral signatures in the VNIR that can be used for their identification. This study summarizes the spectral features of hydrous chlorides and proposes a methodology to detect these minerals in CRISM data. Preliminary application of these methods shows they may be useful to distinguish chlorides from other aqueous minerals.

Methods: *Spectral Features of Hydrous Chlorides.*

We studied the following minerals: antarcticite ($CaCl_2 \cdot 6H_2O$) [7,8], bischofite ($MgCl_2 \cdot 6H_2O$) [7-9], carnallite ($KMgCl_3 \cdot 6H_2O$) [7], halite (NaCl) [7], hanksite ($Na_{22}K(SO_4)_9(CO_3)_2Cl$) [10], hydrohalite ($NaCl \cdot 2H_2O$) [8], kainite ($KMg(SO_4)\,Cl \cdot 3H_2O$) [7], sinjarite ($CaCl_2 \cdot 2H_2O$) [7,8], sylvite (KCl) [10], calcium chloride tetrahydrate ($CaCl_2 \cdot 4H_2O$) [7,8], and magnesium chloride ($MgCl_2$) [9] in different hydration states. Band positions for each minerals were derived from literature [7-9] or were obtained from the absorption positions of USGS lab spectra data observed in the ENVI program (hanksite and sylvite) [10] (Fig. 1).

CRISM parameter values associated with anhydrous and hydrous chloride absorption features were calculated for each laboratory mineral spectrum using equations from [11]: BD1400, BD1500_2, BD1750_2, BD1900_2, BD1900r2, BD2100 (where BD is the strength of the depth of the band at the specified wavelength) and SINDEX2 (sulfate index). For comparison, we calculated the same parameters for a selection of sulfates (kieserite, melanterite, jarosite, hexahydrite, ferricopiapite, szomolnokite, schwertmannite, gypsum, and anhydrite), anhydrous carbonates (kalicinite, calcite 09/10, magnesite a/b, siderite a/b, nahcolite a/b, and pokrovskite), and phyllosilicates (illite, montmorillinite, saponite, smectite, serpentine, nontronite, kaolinite, chlorite and palagonite) reported or suspected to be associated with chloride deposits. The resulting values for each mineral group were compared to determine parameters that are most useful to distinguish each group.

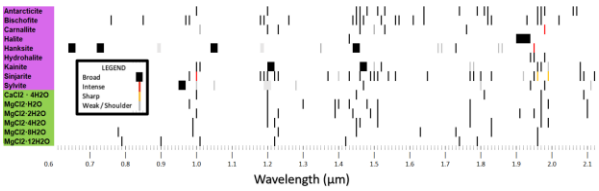

Fig. 1: *Chloride minerals and the positions of their associated absorptions at different wavelengths collected from literature and lab spectra.*

CRISM analysis. CRISM Targeted Reduced Data Record (TRDR) hyperspectral images were collected at 40 sites where chlorides have been most confidently identified by THEMIS [1] and previous CRISM surveys [2]. The CRISM images underwent atmospheric corrections, before observations of the spectra began, using the CRISM Analysis Tool (CAT). Using the ENVI software we produced RGB color schemes of the chloride-relevant parameters: BD1400, BD1500_2, BD1750_2, BD1900_2, BD1900r2, BD2100, and SINDEX2 [11], to evaluate their usefulness to detect chlorides.

Results & Discussion: Table 1 summarizes the CRISM parameter values of chlorides and associated minerals and was used to determine which parameters were most useful to distinguish the groups. We find that BD1500_2, BD1750_2, BD 1900_2 and BD2100_2 were most useful to isolate the anhydrous chlorides from other mineral groups and hydrous chlorides (Figs. 2 and 3).

Table 1: *The highlighted sections represents parameters used in this study. '+' marks signifies calculated values above 0, '-' signifies calculated values below 0, and a label of 0 was used if a value of 0 was produced. The topmost orange labeled row (?) indicated hydrous chlorides and where the calculated value plots.*

	BD1400	BD1500_2	BD1750_2	1900_2	1900r2	2100	BD2210_2	MIN2200	SINDEX2
Chlorides	-	+	+	++	++	-	vary	-	+
Phyllosilicates	+	-	-	+	+	-	vary	0	-
Anhy Carbonat	+	-	-	+	vary	-	0	0	-
Gypsum	-	+	++	+	+	+	+	?	+
Jarosite	-	0	-	+	?	0	?	?	-

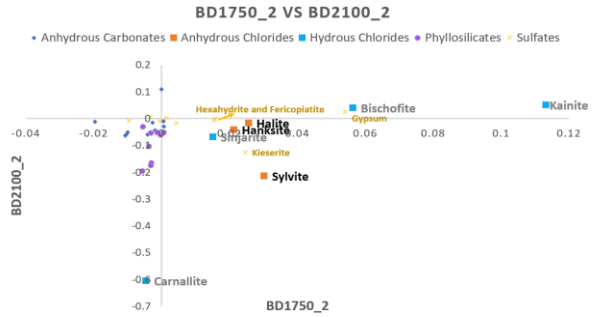

Fig. 2. *Parameter plot using the BD1750_2 parameter versus the BD2100_2 parameter as defined in [11] .*

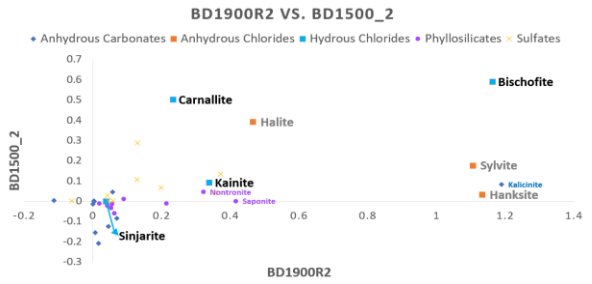

Fig. 3. *Parameter plot using the BD1900r2 parameter versus the BD1500_2 parameter as defined in [11].*

The plots typically contained a few outliers and in response we developed a rationale to ascertain plots that were not sensitive to clay minerals such as the phyllosilicates, plotted in close proximity to the chlorides. Fig. 2 displays an isolation of chlorides from the phyllosilicates (purple circles) which proves that parameters BD1700_2 and BD2100_2 will have greater influence on detecting chloride minerals in a RGB manipulated CRISM image. Furthermore the plot exemplifies that carnallite, bischofite, and kainite are not clustered amongst the anhydrous chlorides. The anhydrous chlorides occur at lower BD1750 values while some hydrous chlorides occur at higher BD1750 values. In Fig. 3 kainite intermixes with both sulfates and phyllosilicates, but remains isolated from the anhydrous chlorides. Sinjarite is the most extreme outlier within the Fig. 3 plot, but remains grouped with the other chloride minerals. In this case the BD1900R2 helps to further separate out the hydrous chlorides occurring at low BD1900R2 values differing from the anhydrous chlorides depicted at higher BD1900R2 values. A cluster can be formed from carnallite, kainite and sinjarite, but bischofite is extraneous at a higher BD1900R2 value. This shows promise for depicting an RGB color scheme that will have stronger hydrous chloride signatures.

Applying these parameters to the CRISM image (Fig. 4) allows for a visual aid that indicates the dissimilarities between the two. Such dissimilarities confirms that the parameters chosen for the anhydrous chlorides will alleviate confusion and ambiguous results on which type of chloride has been identified using CRISM images.

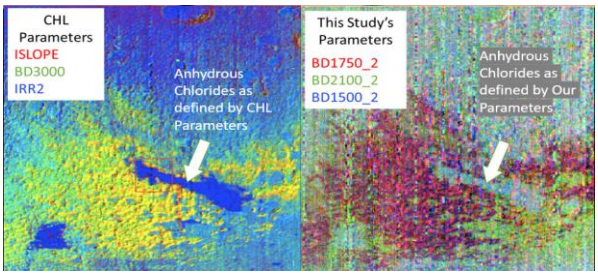

Fig. 4: *This study's parameters indicate the anhydrous chlorides (right) have a similar sensitivity to chlorides as the MICA Files prescribed CHL parameter to detect anhydrous chlorides (left) in CRISM RGB schemed images.*

Conclusion: In the VNIR, we find that chlorides typically have higher values of BD1500_2 and BD1750_2 than phyllosilicates and anhydrous carbonates from the chlorides in general. The BD2100 parameter further helps to differentiate the chlorides from some sulfates.

Hydrous chlorides typically have higher values of BD1750_2 and BD1500_2 than anhydrous chlorides. Although both types of chlorides have elevated BD1900r2 features in our survey, truly anhydrous chlorides should have lower values than the laboratory spectra.

Acknowledgments: This study was conducted through the LPI Summer Undergraduate Program for Planetary Research (SUPPR) and funded by NASA. Special thanks to the LPI associate Dr. Tracy Gregg and Claudia Bellard as well as Wesleyan University for providing remote access to their resources and facilities. CRISM images were collected through the Planetary Data system.

References: [1] Osterloo M. M. et al. (2010) JGR: Planets 115 (E10). [2] Beck A. W. et al (2019) Icarus 338: 113552. [3] Thomas, N. H. et al. (2019) Geophys. Res. Lett. 46.19: 10754-10763. [4] Lynch K. L., et al. (2015) JGR: Planets 120.3, 599-623 [5] Ruesch O. et al. (2012) JGR: Planets 117 (E11). [6] Seelos K. D. et al. (2019) LPI. No. (2132) 2745. [7] Crowley, J. K. (1991) JGR: Solid Earth, 96(B10), 16231-16240. [8] Thomas, E. C. et al. (2017) ACS Earth and Space Chemistry, 1(1), 14-23. [9] Shi, E. et al. (2020) JRS 51(9), 1589-1602. [10] USGS Library Spectra Kokaly, R. F. et al. (2017) (USGS). [11] Viviano-Beck C. E. et al. (2014) JGR: Planets, 119(6), 1403-1431.